Downloaded from ijeee.iust.ac.ir at 17:48 IRDT on Monday June 25th 2018

# Analyzing the Propagation Behavior of a Gaussian Laser Beam through Seawater and Comparing with Atmosphere

F. D. Kashani[1]*, E. Kazemian [1, 2], M. Reza Hedayati Rad[3]

[1]Photonic Lab, Physics Department, Iran University of Science and Technology, Tehran, Iran

[2] Science Department, Maritime University of Imam Khomeini, Nowshahr, Mazandaran

[3] Electronic Engineering Department, Imam Hosein University, Tehran, Iran

F_dk@iust.ac.ir, e_kazemian@iust.ac.ir, mrheda@gmail.com

0098-21-77240477

*Corresponding author: f_dk@iust.ac.ir

**Abstract**:

Study of the beam propagation behavior through oceanic media is a challenging subject. In this paper, based on generalized Collins integral, the mean irradiance profile of Gaussian laser beam propagation through ocean is investigated. Power In Special Bucket (PIB) is calculated. Using analytical expressions and calculating seawater transmission, the effects of absorption and scattering on beam propagation are studied. Based on these formulae,

Downloaded from ijeee.iust.ac.ir at 17:48 IRDT on Monday June 25th 2018

propagation in ocean and atmosphere are compared. The effects of some optical and environmental specifications, such as divergence angle and chlorophyll concentration in seawater on beam propagation by using mean irradiance, PIB and analytical formula of oceanic transmission are studied. The calculated results are shown graphically.

**Keywords:** Propagation of Gaussian Beams, Absorption and Scattering, Extinction coefficient, Seawater, Mean Irradiance

## 1. Introduction

With the increasing human presence in the seas and oceans, also the development of electro-optics devices based on detection of lights propagating through water, nowadays, investigation of behavior of light propagating through this dynamic fluid has a significant importance. Since humans are limited in their ability to work underwater, Remotely Operated Vehicles (ROVs) and Autonomous Underwater Vehicles (AUVs) have been in service since 1950s to perform underwater tasks, such as collecting data and retrieving items. The mobility requirements of submarines and autonomous underwater vehicles make tethered links infeasible. The radio frequency electromagnetic waves are highly attenuated in ocean water, preventing their wide spread use and acoustic communication are limited in bandwidth. Optical wireless

Downloaded from ijeee.iust.ac.ir at 17:48 IRDT on Monday June 25th 2018

communications that exploit the blue/green transparency window of seawater potentially offer high bandwidth with short-range communications [1-6]. The biggest challenges of underwater optical communications originate from the fundamental characteristics of ocean water. Light sources and detector technologies are relatively well developed on the component level, but there is little information available concerning the use of ocean water as an optical communication media [7, 8]. It is necessary to have a comparison between two media, water and atmosphere, to find similarities and dissimilarities. In this paper, first, analytical formula for intensity distribution of laser diode Gaussian beam, which propagates through optical path in seawater, is derived. In next step, quantitative effects of seawater scattering and absorption as an optical power attenuation factor (transmission function), in the fixed deep, is calculated. It is worth mentioning that the effects of ocean phenomena are classified in two groups: 1- Scattering and absorption, 2- Turbulence (The pressure and temperature gradient and sea waves cause oceanic turbulence and affect optical wave propagation). In this paper, the effects of scattering and absorption are investigated but the effect of turbulence is neglected. After the selection of appropriate wavelength for underwater propagation, the comparison between atmosphere and water attenuation is done. The detector's received power is calculated analytically. Based on the analytical formulae of

Downloaded from ijeee.iust.ac.ir at 17:48 IRDT on Monday June 25th 2018

intensity distribution and optical power, the effects of chlorophyll concentration, initial beam divergence and optical path on propagation behavior are investigated. The related results from calculation and simulation are illustrated by graphs and tables.

## 2. Gaussian beam propagation through ocean

For a Gaussian beam with circular symmetry at the plane $z'$ (distance from beam waist location), the electrical field distribution can be expressed as follows [9]:

$$U_0(\vec{r},0) = A_0 \frac{w_0}{w(z')} \exp\left(-\frac{r^2}{w^2(z')}\right) \exp\left(-jkz' - \frac{jkr^2}{2F_0(z')} + j\xi(z')\right) \quad (1)$$

where $w_0$, $w(z')$ and $F_0(z')$ are beam waist, a measure of the beam width and wave front radius of curvature, respectively. $A_0$ is the field constant amplitude. $\xi(z')$ is longitudinal phase. Propagation of the light electrical field is calculated based on generalized Collins formula as follows [10]:

$$U(\vec{r},z) = \frac{-jk_0}{2\pi B} \exp(jk_0 z) \int_{-\infty}^{\infty}\int_{-\infty}^{\infty} U_0(\vec{\rho},0) \exp\left[\frac{jk_0}{2B}\left(A\rho^2 - 2\vec{\rho}.\vec{r} + Dr^2\right)\right] d^2\rho \quad (2)$$

where $\vec{r}$ and $\vec{\rho}$ are the transverse coordinate vectors at receiver and transmitter planes, respectively. A, B, C and D are ABCD matrix elements of the optical

Downloaded from ijeee.iust.ac.ir at 17:48 IRDT on Monday June 25th 2018

system. The ABCD matrix elements for media with constant refractive index as follow [11]:

$$\begin{bmatrix} A & B \\ C & D \end{bmatrix} = \begin{bmatrix} 1 & \frac{z}{n} \\ 0 & 1 \end{bmatrix} \tag{3}$$

To calculate laser beam intensity distribution, it is nessesary to substitute Eq. (1) in Eq. (2), and solve the related integral using ABCD matrix elements(Eq. (3)). Using the integral results and the cross-spectral density function, $I(\vec{r},z)=\langle U(\vec{r},z)U^{*}(\vec{r},z)\rangle$, the intensity distribution formula is calculated as follows:

$$\begin{aligned} I(\vec{r},z) &= \frac{n^2k_0^2A_0^2w_0^2}{4\alpha\alpha^{*}z^2w^2(z')}\exp\left(\frac{-n^2k_0^2r^2}{2\alpha\alpha^{*}z^2w^2(z')}\right), \\ \alpha &= \frac{1}{w^2(z')}+j\frac{k}{2}\left(\frac{1}{F_0(z')}-\frac{1}{z}\right), k_0=\frac{2\pi}{\lambda_0} \end{aligned} \tag{4}$$

where $\lambda_0$ is vacuum wavelength. Considering this fact that only some part of the receiving power can reach the detector, the received power must be calculated over a circular area with radius “a” as follows [9]:

$$P_a = \int_0^a \int_0^{2\pi} I(\vec{r},z)\, r\, d\phi\, dr \tag{5}$$

where $I(\vec{r},z)$ is intensity distribution in $(\vec{r},z)$. Substituting Eq. (4) into Eq. (5), the power on the surface of optical receiver can be calculated as follows:

$$P = \frac{\pi A_0^2 w_0^2}{2}\left(1-\exp\left(\frac{-k^2 a^2}{2\alpha\alpha^* z^2 w^2(z')}\right)\right) \quad (6)$$

In this calculation, the ocean water effects have not been included. However, in almost all applications, it is necessary to take ocean water effects and transmission function of ocean into the account. In section (3) the ocean transmission function due to absorption and scattering are calculated.

### 3. Ocean water transmission calculation

The basic formula for a typical optical intensity distribution propagating through ocean water is an exponential decaying function, Beer's Law [12]:

$$I(\vec{r},z) = I_0(\vec{r},z)e^{-\alpha(\lambda)z} \quad (7)$$

where $I(\vec{r},z)$ is the intensity distribution after traveling the path length $z$ through the medium with loss, $I_0(\vec{r},z)$ is the intensity distribution without considering medium attenuation, and $\alpha(\lambda)$ is the total attenuation coefficient of the medium. Attenuation underwater is the loss of beam intensity due to both intrinsic absorption by water, dissolved impurities, organic matter and scattering from the water, impurities including organic and inorganic particulates. The amount of attenuation changes with each water type. The total attenuation coefficient of seawater is calculated as follows:



Downloaded from ijeee.iust.ac.ir at 17:48 IRDT on Monday June 25th 2018

Downloaded from ijeee.iust.ac.ir at 17:48 IRDT on Monday June 25th 2018

$$\alpha(\lambda) = a(\lambda) + b(\lambda) \tag{8}$$

where $a(\lambda)$ is spectral absorption coefficient and $b(\lambda)$ is the spectral scattering coefficient. Considering the absorptions of Chlorophyll, fulvic and humic acids, the total absorption coefficient is obtained as follows [4, 7, 13]:

$$\begin{aligned} a(\lambda) = a_w(\lambda) + a_c^0(\lambda)\left(C_c / C_c^0\right)^{0.602} \\ + a_f^0 C_f \exp(-k_f \lambda) + a_h^0 C_h \exp(-k_h \lambda)\left(m^{-1}\right) \end{aligned} \tag{9}$$

where

| | |
|---|---|
| $a_w(\lambda)$ | Absorption coefficient of pure water |
| $a_c^0(\lambda)$ | Specific absorption coefficient of chlorophyll |
| $a_f^0 = 35.959 \frac{m^2}{mg}$ | Specific absorption coefficient of fulvic acid |
| $a_h^0 = 18.828 \frac{m^2}{mg}$ | Specific absorption coefficient of humic acid |
| $C_c$ | The total concentration of chlorophyll in mg/m$^3$ |
| $C_c^0 = 1 \frac{mg}{m^3}$ | |
| $k_f = 0.0189 \, 1/nm$ | |
| $k_h = 0.01105 \, 1/nm$ | |
| $C_f$ | The concentration of fulvic acid |
| $C_h$ | The concentration of humic acid |

For chlorophyll concentrations $0 \le C_c \le 12 \, mg/m^3$, $C_h$ and $C_f$ are as follows [4, 7, 13]:

$$C_f = 1.74098 C_c \exp\left(0.12327\left(\frac{C_c}{C_c^0}\right)\right) \quad (10\text{-a})$$

$$C_h = 0.19334 C_c \exp\left(0.12343\left(\frac{C_c}{C_c^0}\right)\right) \quad (10\text{-b})$$

Scattering can be thought of as the redirection of incident photons into new directions, so it prevents the forward on-axis transmission of photons, thereby casting a shadow. This effect is taken into account as an extinction (Total scattering) coefficient. The total scattering, $b(\lambda)$, is a linear combination of the scattering coefficient of pure water, $b_w(\lambda)$, scattering from small particles, $b_s^0(\lambda)$, as a function of wavelength and concentration, and scattering from large particle, $b_l^0(\lambda)$, as a function of wavelength and concentration. $b(\lambda)$ is:

$$b(\lambda) = b_w(\lambda) + b_s^0(\lambda) C_s + b_l^0(\lambda) C_l \quad (11)$$

where

$C_s$ = Total concentration of small particles

$C_l$ = Total concentration of large particles

$$b_w(\lambda) = 0.005826\left(\frac{400}{\lambda}\right)^{4.322}, b_s^0(\lambda) = 1.151302\left(\frac{400}{\lambda}\right)^{1.7}, b_l^0(\lambda) = 0.3411\left(\frac{400}{\lambda}\right)^{0.3}$$

Adding all three functions together gives:



Downloaded from ijeee.iust.ac.ir at 17:48 IRDT on Monday June 25th 2018

$$b(\lambda) = 0.005826\left(\frac{400}{\lambda}\right)^{4.322} + 1.151302\left(\frac{400}{\lambda}\right)^{1.7} C_s + 0.3411\left(\frac{400}{\lambda}\right)^{0.3} C_l \qquad (12)$$

$$C_s = 0.01739 C_c \exp\left(0.11631\left(\frac{C_c}{C_c^0}\right)\right), C_l = 0.7628 C_c \exp\left(0.03092\left(\frac{C_c}{C_c^0}\right)\right)$$

Using Eqs. (8-12), the ocean water total attenuation coefficient is calculated as a chlorophyll concentration function. Mean chlorophyll concentration is estimated with Satellite Ocean Color Sensor. In 1976, N. G. Jerlov published the book Marine optics that proposed a system for classifying the clarity of the water based on chlorophyll concentration value. This system is still widely used since it is convenient. The various water types are divided into two categories: oceanic (blue water) and coastal waters (littoral zone). The oceanic group is subdivided into 3 groups, type I-III and the coastal groups are subdivided into types 1 through 9. The chlorophyll concentrations in the five different Jerlov Water types are summarized in table (1) and it is the basis of next section calculations and simulations.

Table 1: Chlorophyll concentrations for five different Jerlov Water types [13].

| Jerlov Water type | Concentrations of chlorophyll mg/m$^3$ |
|---|---|
| I | 0.03 |
| IA | 0.1 |
| IB | 0.4 |
| II | 1.25 |
| III | 3 |

Downloaded from ijeee.iust.ac.ir at 17:48 IRDT on Monday June 25th 2018

Downloaded from ijeee.iust.ac.ir at 17:48 IRDT on Monday June 25th 2018

## 4. Results and discussions

In this section, Based on Eqs. (4-12), the calculations related to investigation of the source parameter's effects (Such as initial beam divergence) and environmental factors (such as chlorophyll concentration, optical path length) on propagation properties are done and the results are shown as tables and graphs. Fig. 1a shows the graph of total attenuation coefficient ($m^{-1}$) as $\alpha(\lambda)=a(\lambda)+b(\lambda)$ for five different Jerlov Water types. Fig. 1b shows the transmission values as a function of wavelength and chlorophyll concentration value.

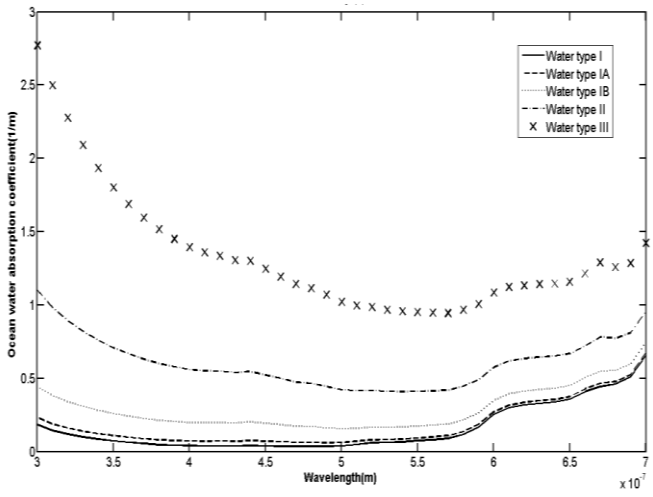


a

Downloaded from ijeee.iust.ac.ir at 17:48 IRDT on Monday June 25th 2018

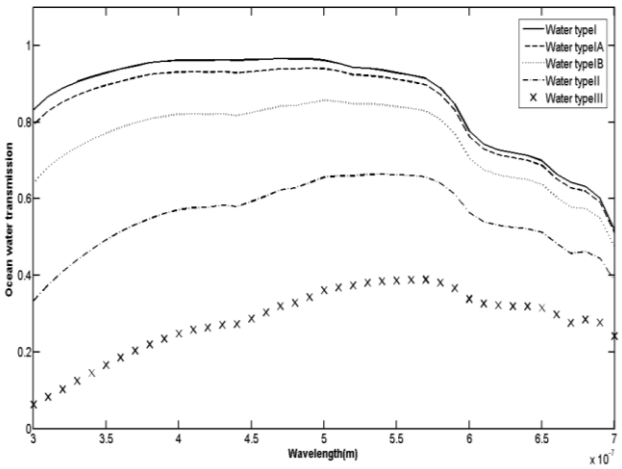


b

Fig. 1: a) The total spectral attenuation coefficient for five Jerlov water types in range 300-700 nm, b) The total transmission for five Jerlov water types in range 300-700 nm.

Table 2 illustrates the amount of five Jerlov water types' transmission coefficients for four different wavelengths.

Table 2: The amount of five different water types transmission for four different wavelengths

| Jerlov Water type | Transmission coefficient (dB/m) λ =405 nm | Transmission coefficient (dB/m) λ =450 nm | Transmission coefficient (dB/m) λ =532 nm | Transmission coefficient (dB/m) λ =632 nm |
|---|---|---|---|---|
| I | -0.17 | -0.16 | -0.27 | -1.42 |
| IA | -0.31 | -0.30 | -0.35 | -1.50 |
| IB | -0.85 | -0.84 | -0.72 | -1.83 |
| II | -2.39 | -2.27 | -1.78 | -2.78 |
| III | -5.89 | -5.42 | -4.20 | -4.59 |

Examining the Fig.1 and table 2 will notice that the minimum for the $\alpha(\lambda)$ shifts to right, from blue region, ~450nm for first two type of Jerlov water, to the more greenish region, ~525nm for water type IB, II and III. The different concentrations of absorptive debris suspended in the different water types cause

Downloaded from ijeee.iust.ac.ir at 17:48 IRDT on Monday June 25th 2018

the shift in wavelength minimum. The loss due to the attenuation coefficient will cause a change in the power reached to the receiver. As $\alpha(\lambda)$ increases, the distance at which the minimum power can be achieve decreases. Therefore, the laser diodes with wavelength 450 nm and 532 nm are selected to compare the propagation through water with atmosphere. similarly, 1550 nm laser diode experiences small amount of attenuation propagating through atmosphere. Based on this fact, transmission coefficient of laser beam with 1550 nm wavelength through some worse weather conditions, dense fog and low visibility, are summerized in table 3.

Table 3: Atmospheric transmission through fog conditions

| Weather condition | Visibility (m) | Transmission coefficient (dB/m) |
|---|---|---|
| Dense fog | 50 | -0.24 |
| Thick fog | 200 | -0.058 |
| Moderate fog | 500 | -0.022 |
| Light fog | 1000 | -0.01 |
| Light mist | 2000 | -0.004 |

Comparing the values in table 2 and 3 shows that atmospheric transmission in the worst case is more than the amount of oceanic water transmission in the best condition. Thus the laser propagation path lenght is about a few tens to several hundred meters, unlike the atmopshere. Laser beam intensity distributions propagating through IA water, in $z = 60\,m$ for four different wavelengths are shown in Fig. 2. The laser source properties are assumed as follows: $\mathrm{P} = 200$ mw, $\theta_0 = 1.5\,mrad$, $w_0 = 1cm$.

Downloaded from ijeee.iust.ac.ir at 17:48 IRDT on Monday June 25th 2018

As mentioned before and based on Fig. 1 and Fig. 2, 450 nm laser diode propagating through I and IA waters have maximum transmission values and minimum attenuation amounts. However, through IB, II and III water with more chlorophyll concentration, 532 nm laser diode experience minimum amount of attenuation.

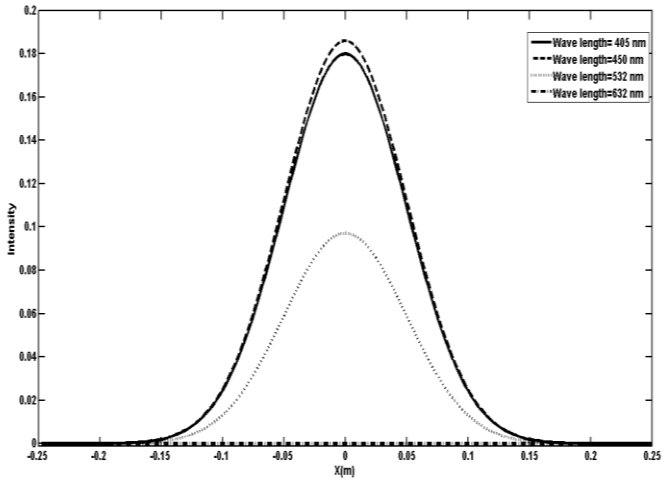


Fig. 2: Intensity distribution in z= 60 m for four different wavelengths through IA water.

Considering this fact, first, propagation properties of 450 nm laser diode through I and IA waters are analyzed, Then, 532 nm laser diode propagation through IB, II and III water types are studied (Fig. 3). Fig. 3 shows intensity distribution for four different wavelengths in $z = 30\,m$. In this figure, laser beam propagates through II water and the other parameters are the same as Fig. 2.

Downloaded from ijeee.iust.ac.ir at 17:48 IRDT on Monday June 25th 2018

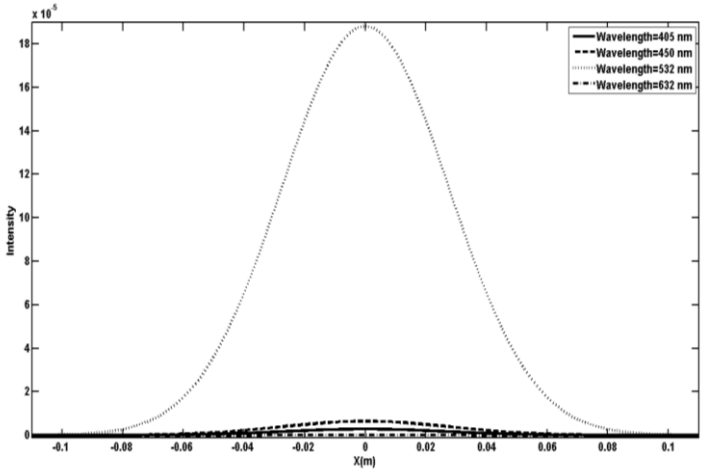


Fig. 3: Intensity distribution in z= 30 m for four different wavelengths through II water.

Fig. 4 shows intensity distributions in three different propagation path lengths. 450 nm and 532 nm laser diodes are investigated in Fig. 4a and 4b, respectively. As it is expected, increasing propagation path length causes an increase in attenuation amount. Fig. 4c shows 450 nm laser diode propagating through IA water type.

Downloaded from ijeee.iust.ac.ir at 17:48 IRDT on Monday June 25th 2018

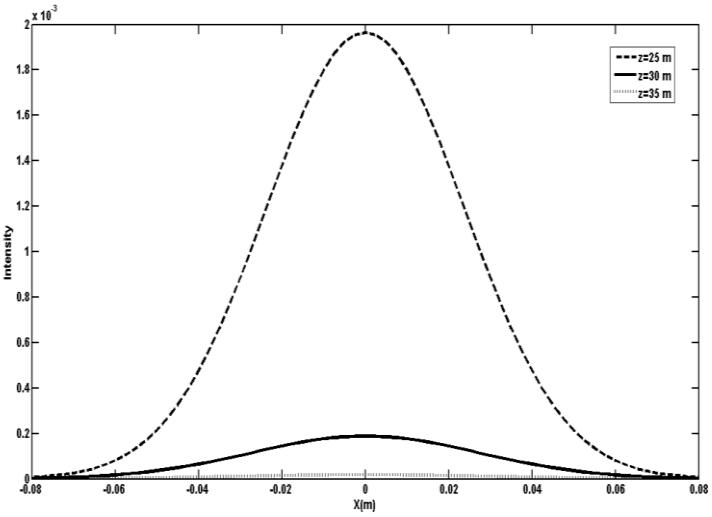


a

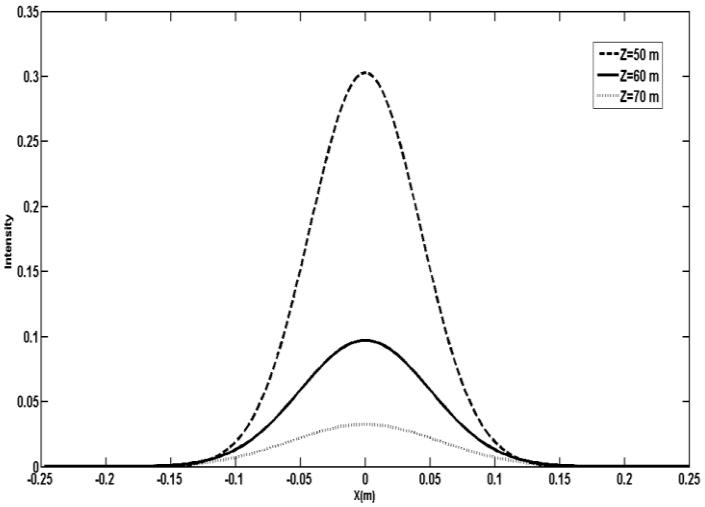


b

Downloaded from ijeee.iust.ac.ir at 17:48 IRDT on Monday June 25th 2018

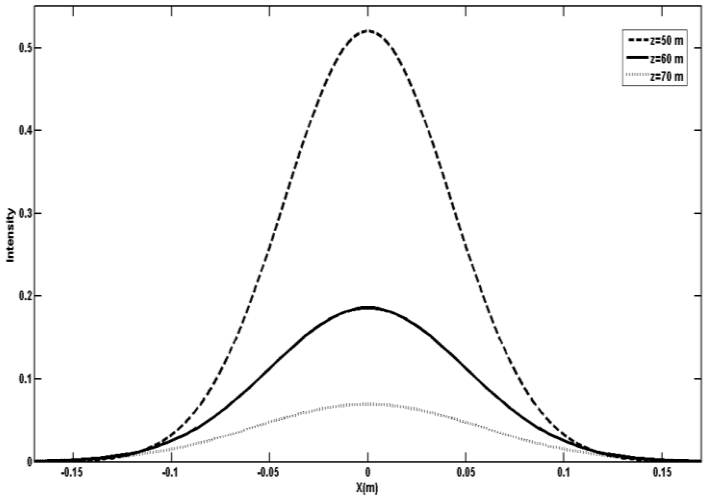


c

Fig. 4: a) Intensity distribution of 450 nm laser beam for three different propagation path lengths through II water, b) Intensity distribution of 532 nm laser beam for three different propagation path lengths through IA water, c) Intensity distribution of 450 nm laser beam for three different propagation path lengths through IA water.

Propagation behaviors of laser diode with different initial beam divergence are the same as propagation properties through atmosphere. Fig. 5 illustrates this phenomenon. Any increase in initial divergence angle causes an increase in beam spatial broadening.

Downloaded from ijeee.iust.ac.ir at 17:48 IRDT on Monday June 25th 2018

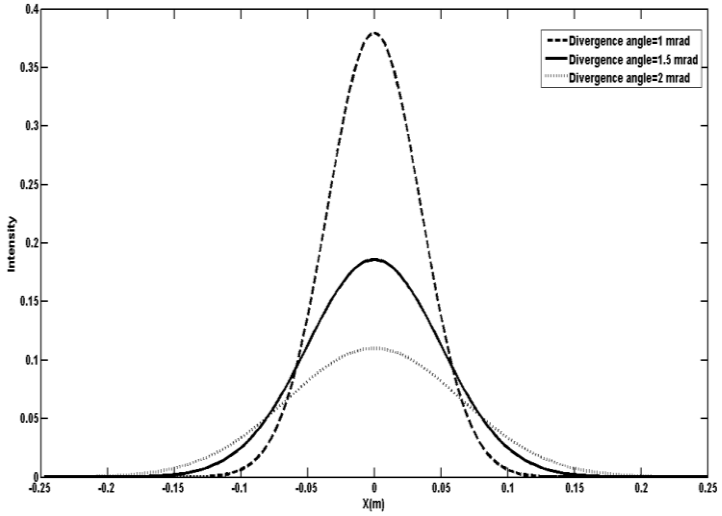


Fig. 5: Intensity distribution in z= 60 m for three different initial beam divergence.

The propagation properties of laser diode with $\lambda$=532 *nm* in different water conditions are the same as 450 nm laser diode in IA water type. Any increase in chlorophyll concentration causes an increase in attenuation due to absorption and scattering and leads to reduction in intensity peak value. Fig. 6 shows the effect of chlorophyll concentration variation. Fig. 6a shows this effect on 450 nm laser beam. Chlorophyll concentration variation influence for 532 nm laser diode is shown in Fig. 6b.

Downloaded from ijeee.iust.ac.ir at 17:48 IRDT on Monday June 25th 2018

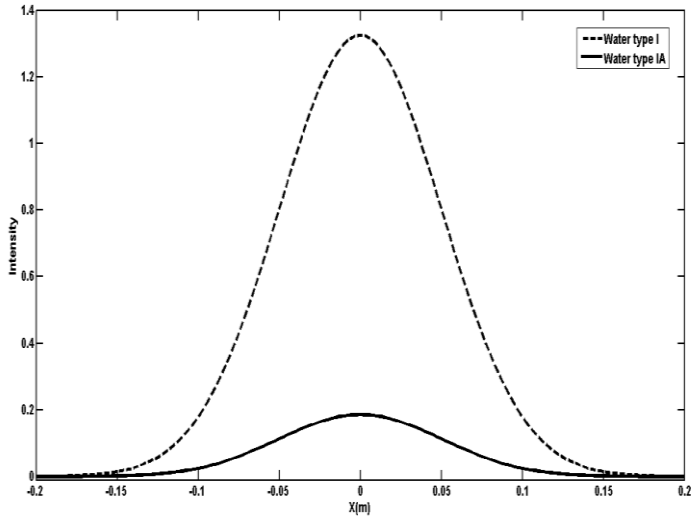


a

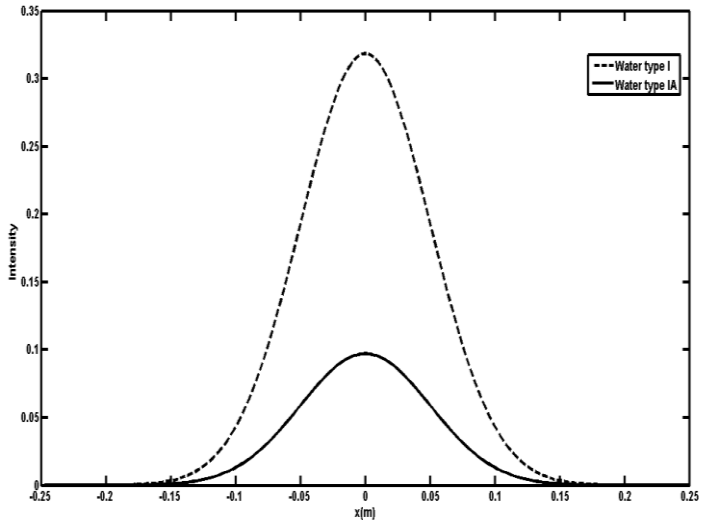


b

Fig. 6. a) Intensity distribution of 450 nm laser diode for two different Jerlov water types, b) Intensity distribution of 532 nm laser diode for two different Jerlov water types.

Downloaded from ijeee.iust.ac.ir at 17:48 IRDT on Monday June 25th 2018

In Fig. 6, as it is expected, increasing chlorophyll concentration causes a decrease in intensity peak values and this behavior is the same for both wavelengths. Fig. 7 shows the intensity distribution of 532 nm laser diode propagating through IB, II and III water types. As it is shown, propagation behavior through IB, II and III waters are the same as I and IA water types. As it is mentioned, the amounts of attenuation are different for IB, II and III Jerlov water types.

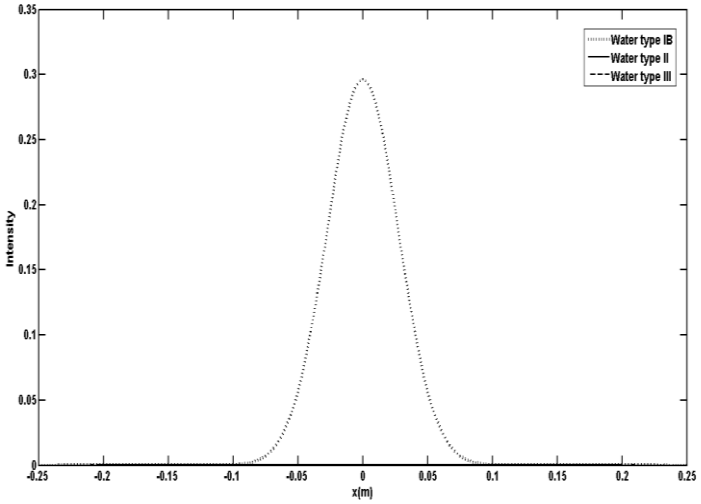


a

Downloaded from ijeee.iust.ac.ir at 17:48 IRDT on Monday June 25th 2018

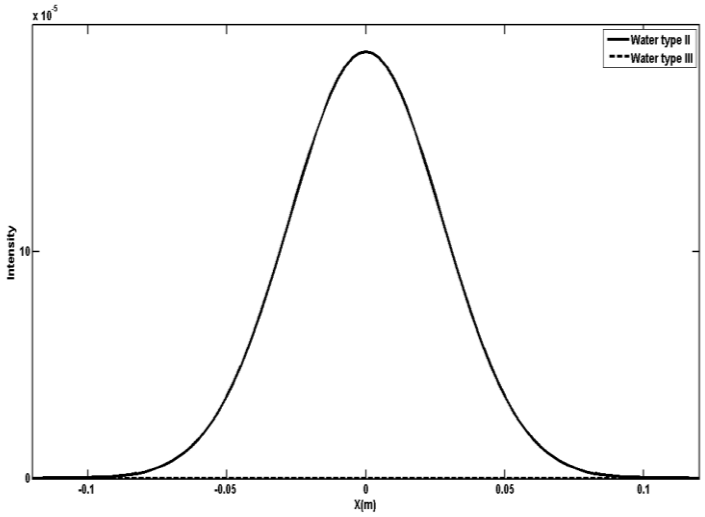


b

Fig. 7: a) Intensity distribution in three water types with different chlorophyll concentration values, b) Intensity distribution in two water types with different chlorophyll concentration values

The other important factor in propagation behavior investigation is received power of the detector. The amount of received power with 20 cm diameter's detector for 450 and 532 nm laser diodes propagating through different water types are summarized in table 4.

Downloaded from ijeee.iust.ac.ir at 17:48 IRDT on Monday June 25th 2018

Table 4: Received power for two different laser diode wavelengths

| Water type | Received power for 532 nm (dBm) | Received power for 450 nm (watt) |
|---|---|---|
| I | 14.94 | 18.10 |
| IA | 12.37 | 13.83 |
| IB | 1.48 | -2.09 |
| II | -30.37 | -45.10 |
| III | -102.61 | -139.53 |

Based on above mentioned calculations, in I and IA water types, the 450 nm laser diode attenuation values are lower than 532 nm ones. However, through IB, II and III water types, 532 nm laser beams experience less attenuation. Results of table 4 indicate this behavior. For two water types, I and IA types, the amount of received power values for 450 nm wavelengths are more than 532 nm lasers. However, for 532 nm laser beams the amounts of received power in IB, II and III Jerlov waters are higher than the other wavelength received power values in the same conditions. Fig. 8 shows variation of received power values versus propagation path length for two wavelengths, 450 nm and 532 nm, through different water types.

As it is shown in Fig. 8, increasing propagation path length causes an increase in laser and water interaction and consequently a decrease in water transmission. This transmission reduction leads to decrease in the amount of received power by increasing optical path length.

Downloaded from ijeee.iust.ac.ir at 17:48 IRDT on Monday June 25th 2018

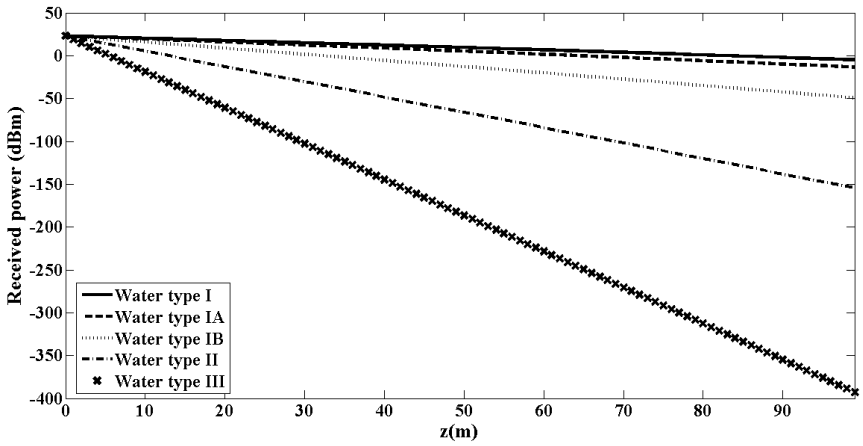


a

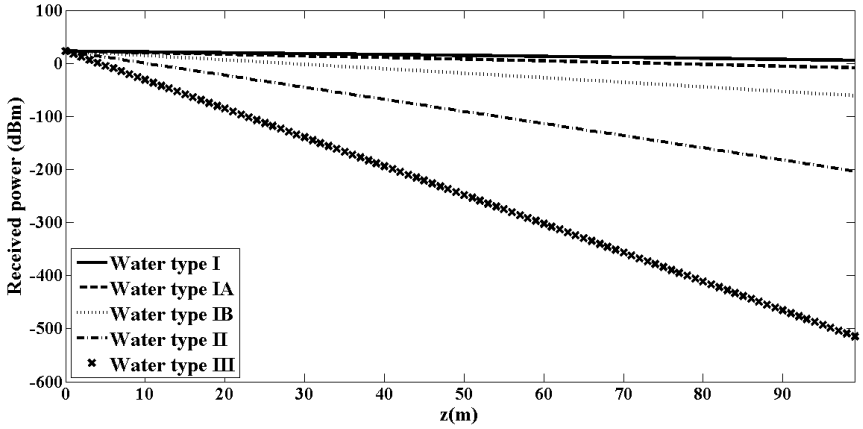


b

Fig. 8. a) Received power values versus propagation path length for 532 nm laser, b) Received power values versus propagation path length for 450 nm laser

The other parameter, which can have significant effects on propagation behavior, is initial beam divergence. Fig. 9 shows the effects of initial source divergence on received power which the 450 nm laser beam propagates through IA water types.

Downloaded from ijeee.iust.ac.ir at 17:48 IRDT on Monday June 25th 2018

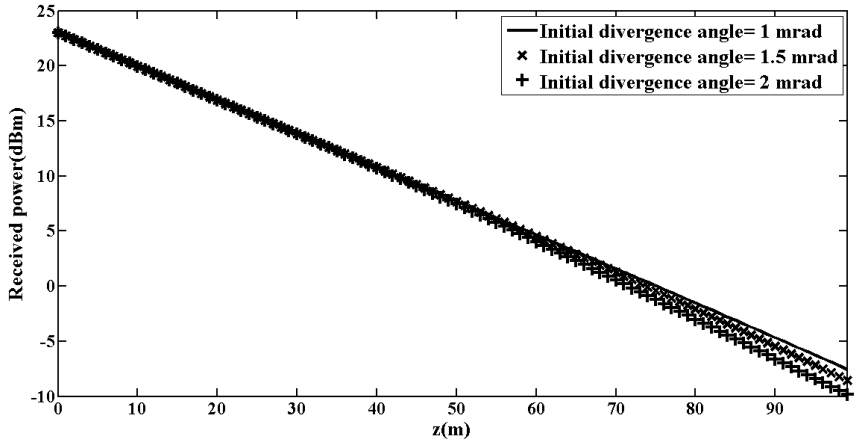


Fig. 9: Received power for three different initial beam divergence

It is clear that due to the short propagation path length and small value of divergence angle, divergence value has no significant effect on received power values. It is worth mentioning that in the other situations- such as longer propagation path length, larger initial divergence angle or smaller aperture diameter- this behavior changes.

## 5. Conclusions

The absorption and scattering of laser beams through ocean water have a significant effect on the performance of imaging and communication systems. Therefore, investigation of propagation behavior is very important. In this paper, analytical formula for intensity distribution on receiver plane is derived. By considering transmission of atmosphere and water, the effects of water

attenuation is compared with atmospheric attenuation. Also, the effects of initial beam divergence and chlorophyll concentration are investigated and it is clarified that: 1- The laser beams with different divergenc values experience different amount of spreading as same as propagation behavior through atmospher. However, divergence has no strong influence on received power due to short propagation path length and small amount of divergence. 2- Any increase in chlorophyll concentration causes a decrease in the amount of water transmission which leads to decrease in intensity peak and received power values. 3- Water transmission values through I and IA waters are lower in 450 nm wavelength. 532 nm laser diode propagation through IB, II and III water types experience less attenuation. 4- As it is expected, increasing optical path length causes an increase in attenuation values.

Downloaded from ijeee.iust.ac.ir at 17:48 IRDT on Monday June 25th 2018

## 6. References

[1] Schill F.; Zimmer U. R. and Trumpf J., "Visible Spectrum Communication and Distance Sensing for Underwater Application", In Proceedings of Australasian Conference Robotics and Automation, Canberra, Australia, December (2004).

[2] Hanson F., Radic S., "High bandwidth underwater optical communication", Applied Optics, Vol. 47, No. 2, pp. 277-283 (2008).

Downloaded from ijeee.iust.ac.ir at 17:48 IRDT on Monday June 25th 2018

[3] Giles J. W. and Bankman I. N., "Underwater optical communications systems. Part 2: basic design considerations", In Proceedings of MILCOM 2005, IEEE Military Communications Conference (IEEE, 2005), pp. 1700-1705. (2005)

[4] Mobley C. D., *Light and Water: Radiative Transfer in Natural Waters* (Academic, 1994).

[5] Cox W., "A 1 Mbps underwater communication system using a 405 nm laser diode and photomultiplier tube", North Carolina State University, Master of Science (2007).

[6] Brundage H., "Designing a wireless underwater optical communication system", Massachusetts Institute of Technology, Master of Science (2010).

[7] Simpson J., "A 1 Mbps underwater communications system using LEDs and photodiodes with signal processing capability", North Carolina State University, Master of Science (2007).

[8] Jaruwatanadilok S., "Underwater wireless optical communication channel modeling and performance evaluation using vector radiative transfer theory", IEEE Journal on Selected Areas in Communications, Vol. 26, No. 9, pp. 1620-1627 (2008).

[9] Saleh LB. E. A. and Teich M. C., *Fundamentals of photonics*, Second edition (Wiley series in pure and applied, New Jersey, 2007).

[10] Andrews L. C. and Phillips R. L., *Laser beam propagation through random media*, Second edition (SPIE optical Engineering press, Bellingham, Washington USA, 2005).

[11] A. E. Siegman, *Lasers* (University Science Books Mill Valley, California, 1986).

[12] Kvicala R., Kvicera V., Grabner M. and Fiser O., "BER and availability measured on FSO link", Radioengineering, Vol. 16, pp. 7-12 (2007).

[13] Chancey M. A., "Short range underwater optical communication links", North Carolina State University, Master of Science (2005).

Downloaded from ijeee.iust.ac.ir at 17:48 IRDT on Monday June 25th 2018